



HAL
open science

Water Control in Producing Wells: Influence of an Adsorbed-Polymer Layer on Relative Permeabilities and Capillary Pressure

Patrick Barreau, Henri Bertin, Didier Lasseux, Philippe Glenat, Alan Zaitoun

► **To cite this version:**

Patrick Barreau, Henri Bertin, Didier Lasseux, Philippe Glenat, Alan Zaitoun. Water Control in Producing Wells: Influence of an Adsorbed-Polymer Layer on Relative Permeabilities and Capillary Pressure. SPE Reservoir Engineering, 1997, 12 (04), pp.234-239. <10.2118/35447-PA>. <hal-03827884>

HAL Id: hal-03827884

<https://hal.science/hal-03827884v1>

Submitted on 2 Dec 2022

HAL is a multi-disciplinary open access archive for the deposit and dissemination of scientific research documents, whether they are published or not. The documents may come from teaching and research institutions in France or abroad, or from public or private research centers.

L'archive ouverte pluridisciplinaire **HAL**, est destinée au dépôt et à la diffusion de documents scientifiques de niveau recherche, publiés ou non, émanant des établissements d'enseignement et de recherche français ou étrangers, des laboratoires publics ou privés.



Distributed under a Creative Commons CC BY 4.0 - Attribution - International License

Water Control in Producing Wells: Influence of an Adsorbed-Polymer Layer on Relative Permeabilities and Capillary Pressure

Patrick Barreau,* Henri Bertin, SPE, and Didier Lasseux, U. of Bordeaux; Philippe Glénat, SPE, Total;
and Alan Zaitoun, SPE, Inst. Français du Pétrole

Summary

To determine modifications of oil/water two-phase-flow properties after injection of water-soluble polymers, unsteady-state flow experiments were performed on both water- and oil-wet (silane-treated) sandstones. The same imbibition cycle (water displacing oil) under the same conditions was performed on the same core, first without any polymer and then after polyacrylamide had been adsorbed within the core. The capillary pressure was measured directly along the core by use of water- and oil-wet semipermeable membranes, while relative permeabilities were determined from the measurement of the saturation profile (by gamma ray absorption), outlet fluid production, and pressure drop.

The action of adsorbed polymer on relative permeabilities was found to be the same with both water- and oil-wet cores (i.e. a selective reduction of the relative permeability to water with respect to the relative permeability to oil). The trend was somewhat different for the capillary pressure. For the case of water-wet sandstones, the capillary pressure remained positive but increased dramatically after polymer adsorption. Because the polymer has little effect on the interfacial tension (IFT), this effect was attributed to the reduction of pore-throat size caused by macromolecule adsorption and to a possible improvement of the wettability of the core to water. For the case of oil-wet sandstone, the capillary pressure curve moved from negative to positive values, indicating that, in addition to pore-size restriction, the wettability of the core changed after polymer adsorption. This wettability change also induced a dramatic drop in residual oil saturation (ROS).

Introduction

Excessive production of water as a result of heterogeneities or fractures often causes channeling or water coning and is a problem of central importance for field operators. Several techniques have been developed to overcome this problem. Among them, direct injection of polymer or gels in the production well was shown to enable the reduction of the water cut. If the drawdown on the treated well can be increased, then, in addition to the reduction in water production, the treatment can induce an increase in oil production.¹ Several re-searchers have studied the mechanisms involved in the action of polymer or gels (Schneider and Owens,² Zaitoun and Kohler,³ Zai-toun *et al.*,⁴ Liang *et al.*⁵). They all found that polymer or gels are able to reduce selectively the relative permeability to water with respect to the relative permeability to oil. Provided that the polymer is hydrophilic, this property does not depend on the polymer type (polyacrylamide, xanthan or scleroglucan) or on the nature of the rock (sandstone, limestone, or unconsolidated sand). Most existing experiments have been performed either under steady- or unsteady-state conditions at a high flow rate (Welge method).

Several physical processes have been proposed to explain the selective action of the polymer. The following are some principal ones.

1. Shrinking of the gel in the presence of oil. Dawe and Zhang⁶ observed water eviction from a gel during the displacement of an oil droplet in a micromodel. The influence of the wettability was also investigated. The gel was shown to have a lower blocking efficiency in oil-wet micromodels.

2. Partitioning of fluids. This hypothesis, put forward by Liang *et al.*,⁵ suggests that a segregation of oil and water occurs in the core and explains the disproportionate permeability.

3. Wall effect. The presence of the polymer adsorbed on pore walls may induce a lubrication effect that favors the flow of oil through the center of the pore channels and attenuate pore-wall roughness. This hypothesis was suggested by Zaitoun and Kohler.³ These authors proposed a simple two-phase-flow capillary model within a cylindrical geometry to describe the effect of an adsorbed polymer layer at the pore wall. To complete this pore-level study, we are developing a numerical model where the pore consists in a periodic two-dimensional (2D) divergent/convergent channel.⁷ The first results⁸ confirm qualitatively the experimental observations.

4. Wettability effect. The adsorption of the hydrophilic polymer on pore walls may enhance the water wettability of the rock and thus contribute to the relative permeability modification.

Most of reported studies were focused on relative permeability modifications, but little information (Barrufet and Ali⁹) is available about the effect of polymer on the capillary pressure. Our experimental procedure aimed at the measurement of this parameter as well. We performed unsteady-state core-flow experiments at low flow rates. To our point of view, these experiments are more realistic than steady-state ones. During these experiments, we measured directly the capillary pressure along the core using semipermeable membranes at pressure taps, and we determined the relative permeabilities over the whole saturation range.

Experimental

Fluids. We used synthetic brines containing 50 g/L⁻¹ KI and 0.4 g/L⁻¹ NaN₃. The potassium ion prevents clay migration while the iodide ion improves the accuracy of saturation measurements by gamma ray attenuation technique.¹⁰ Sodium azide was used as a bactericide. As the oil phase, we used Marcol 52, a mineral oil having a viscosity of 10.5 mPa·s at 20°C. IFT's between brine and oil and between polymer solution and oil were measured with the ring technique; values were 33×10^{-3} and 28×10^{-3} N/m⁻¹, respectively.

Polymer Solution. We used a high-molecular-weight nonionic polyacrylamide (PAM) available in powder form. The polymer behaves like a flexible coil in solution with an average diameter of 0.32 μ m. Its molecular weight is 9×10^6 dalton.⁴ The solution, whose concentration is 2500 ppm, was prepared by slow addition of polymer powder to the brine in a vortex created by magnetic stirring. After complete dissolution of the powder, the solution was filtered on line with a set of 8-, 3- and 1.2- μ m Millipore membranes to remove any solid or microgel. The viscosity of the polymer solution was measured over a wide range of shear rates with a Contraves LS 30 viscometer. The curve of viscosity vs. shear rate is plotted in Fig. 1.

Core Samples. Both water- and oil-wet media were used in this study.

Water-Wet Medium. The water-wet medium is a Vosges sandstone ("gray" quality) with a permeability ranging between 0.25 and

*Now at Inst. Français du Pétrole.

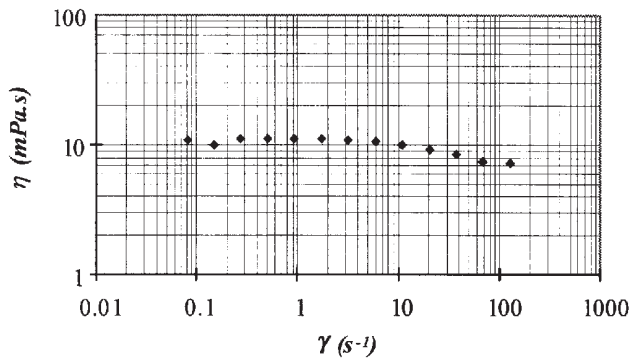


Fig. 1—Viscosity of PAM solution (2500 ppm).

$0.75 \mu\text{m}^2$ and a porosity ranging between 0.23 and 0.25. This sandstone, used in several experimental studies,^{11,12} is strongly water-wet and relatively homogeneous. The mineralogy was determined by X-ray diffraction. The sandstone was mainly composed of quartz, feldspars, and clays (mainly magnesite, chlorite, and some traces of illite and kaolinite). Clay content of the rock is approximately 7%. The specific area ($A = 3.25 \text{ m}^2/\text{g}^{-1}$) was measured by nitrogen adsorption. Microscopic examination of the rock showed that the sand grains are almost totally covered by clays. Pore-size distribution was determined by mercury injection (Purcell method—Fig. 2). Average pore radius is $8.5 \mu\text{m}$.

Oil-Wet Medium. The oil-wet medium was obtained by silanation of the same Vosges sandstone. The method consists of grafting silane molecules to the surface of the rock, substituting silanol hydrophilic groups by organosilyl hydrophobic groups. This treatment was used by several authors^{13,14} and found to be stable after oil or brine flow. This chemical treatment changes the wettability of the porous medium and produces a homogeneous hydrophobic layer on the surface of the solid without affecting the other petrophysical properties, like porosity or permeability. This treatment does not correspond to a natural wettability change of the rock; however, it provides a reliable laboratory core with properties that can be compared with the ones of the original material.

Sandstone cores had a $5 \times 5\text{-cm}^2$ cross section and were 20 cm long. Cores were wrapped in an epoxy resin reinforced with glass-fiber to ensure enough tightness and sufficient transparency for gamma ray measurements. The capillary pressure was measured with micro-pore water- and oil-wet membranes placed at the bottom and upper sides of the horizontal core, respectively. Those membranes were changed after polymer injection to avoid plugging problems.

Core-Test-Equipment

Our experimental flow equipment, represented in Fig. 3, was made of a displacement pump connected to the oil, brine, and polymer-solution containers. The core sample was positioned on a 2D rig displacing a gamma ray source. A photon-counting device was used to measure the saturation. Pressure drop across the core and capillary pressure at three different levels along the core were measured with pressure transducers. During two-phase-flow experiments, cumulative volumes of oil and water were determined on the effluents by use of a graduated cell on a scale.

The saturation measurements were performed at 60 points located on a 4×15 grid (illustrated in Fig. 3). The beam was collimated at a diameter of 4 mm. The photon-counting time for each measurement was 25 seconds so that the entire saturation field was determined in less than 30 minutes. We calculated the average saturation (computed with four saturation measurements) on the 15 straight sections of the core. Displacement of the 2D rig and data acquisitions of saturation, pressure drop, capillary pressure and effluent recovery were monitored by a personal computer. The system temperature was kept constant at $20 \pm 1^\circ\text{C}$.

Experimental Procedure. Flow tests, with both water- and oil-wet media, were run with the following sequences.

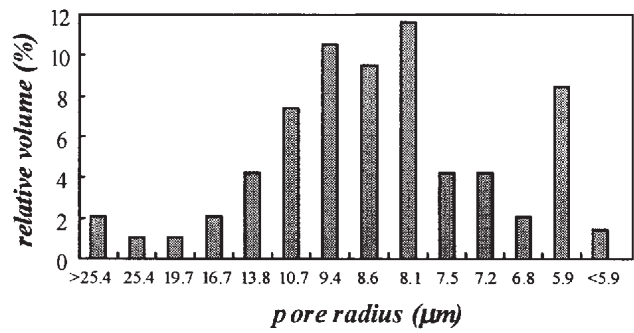


Fig. 2—Pore-size distribution obtained by Purcell method.

1. Saturation of the core under vacuum with brine. Measurement of pore volume, porosity and permeability.
2. First oilflood at high flow rate ($q = 120.10^{-6} \text{ m}^3/\text{h}$). Measurement of S_{wi}^1 and k_o at S_{wi}^1 .
3. Installation of the semipermeable membranes used to measure the capillary pressure.
4. First waterflood performed at low flow rate ($q = 5.10^{-6} \text{ m}^3/\text{h}$). Measurement of water saturation, pressure drop, and oil recovery evolution with time. Pressure difference between oil- and water-wet membranes was monitored while measuring the saturation evolution. This measurement provides the capillary pressure vs. water saturation. At the end of the waterflood we measured S_{or}^1 and k_w at S_{or}^1 .
5. Low-shear injection of 2 PV of polymer followed by a shut-in time of 12 hours to complete polymer adsorption. Measurement of polymer adsorption from the delay of the polymer front after 1 PV has been injected.
6. Waterflood ($q = 5.10^{-6} \text{ m}^3/\text{h}$) to displace the nonadsorbed polymer remaining in the core. Measurement of S_{or}^2 and k_w at S_{or}^2 .
7. Change semipermeable membranes plugged by polymer.
8. Second oilflood ($q = 120.10^{-6} \text{ m}^3/\text{h}$). Measurement of S_{wi}^2 and k_o at S_{wi}^2 .
9. Second waterflood ($q = 5.10^{-6} \text{ m}^3/\text{h}$). Measurement of S_{or}^3 and k_w at S_{or}^3 .

Results and Discussion

Our experimental results are presented in terms of modification of capillary pressure and relative permeabilities caused by the polymer adsorbed in the core. Because of the high flow rate used during drainage cycles, measurements of saturation fields vs. time were not performed during this stage of the experiment and were focused on the imbibition cycles (water displacing oil).

The capillary pressure was measured directly at each tap level. Because the saturation of the core was also checked at the same tap level, we could establish capillary pressure curves vs. saturation. Pressure was recorded continuously, every minute, while the saturation was measured with a time lag of 30 minutes. As a consequence, the capillary pressure relationship contains a limited number of points corresponding to pressure and saturation measurements at

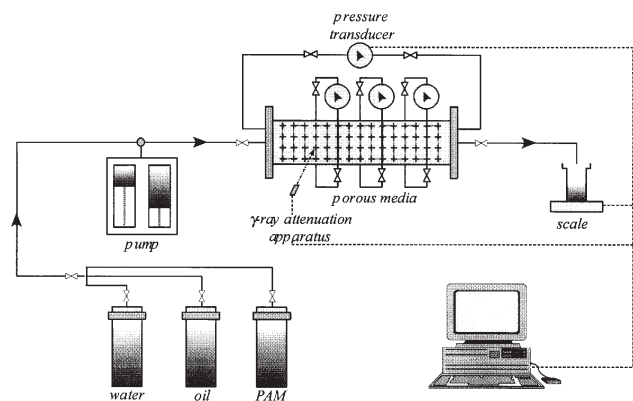


Fig. 3—Experimental setup.

TABLE 1—WATER-WET CORE: ENDPOINT DATA BEFORE AND AFTER POLYMER

ϕ	0.23
$k, \mu\text{m}^2$	0.25
S_{wi}^1	0.327
k_o at $S_{wi}^1, \mu\text{m}^2$	0.222
S_{or}^1	0.336
k_w at $S_{or}^1, \mu\text{m}^2$	0.0155
S_{or}^2	—
k_w at $S_{or}^2, \mu\text{m}^2$	—
S_{wi}^2	0.492
k_o at $S_{wi}^2, \mu\text{m}^2$	0.138
S_{or}^3	0.328
k_w at $S_{or}^3, \mu\text{m}^2$	0.0007

the same instant and the same position. A similar method was used successfully by Kalaydjian.^{15,16}

Relative permeabilities were determined with a minimization computer program, FISOLE™¹⁷ from one-dimensional experimental values of local saturation, outlet production, and pressure drop. The capillary pressure curve was used as input data. Simultaneous determination of relative permeabilities and capillary pressure from experimental data was performed as well and provided good results. Results obtained with both water- and oil-wet media are presented next.

Water-Wet Medium. Table 1 summarizes the experimental data.

Polymer Adsorption. The polymer front, determined by viscosity measurements in the Newtonian regime, is represented in Fig. 4. The delay of the front with respect to 1 PV provides a value of 97 $\mu\text{g}/\text{g}$, which is in good agreement with previous results.³ The thickness of the adsorbed-polymer layer was estimated from the permeability reduction to brine at ROS. To estimate the polymer-layer thickness, h , we used the classic model of a bundle of capillary tubes for the porous medium. Assuming that the polymer layer is impervious, we obtain^{3,18}

$$h = \left(1 - R_k^{-1/4}\right) \sqrt{\frac{8kk_{rw}}{\phi(1 - S_{or}^3)}} \quad \dots \dots \dots (1)$$

In this equation, the permeability reduction, R_k = ratio of effective permeability to water at ROS before and after polymer adsorption. In our case, we found $h = 0.49 \mu\text{m}$, a value which is also in good agreement with previous results.³

Capillary Pressure. The capillary pressure, measured as described earlier during the two successive imbibition cycles (Steps 4 and 9) are plotted in Fig. 5. We observe a strong increase in the irreducible water saturation after polymer adsorption—from $S_{wi}^1 = 0.327$ to $S_{wi}^2 = 0.492$. This difference can be understood as a result of the adsorbed-polymer layer, which traps an extra amount of brine (this actually represents a weak contribution) and closes smaller pores to oil flow. At the end of the two imbibition cycles, the ROS is almost unchanged (see S_{or}^1 and S_{or}^3 in Table 1). The capillary pressure is strongly increased over the whole saturation range by the presence of adsorbed polymer in the core.

From our point of view, because brine/oil and polymer-solution/oil IFT's are almost the same, this behavior can only be explained by an improvement of the wettability on the one hand and a net-pore-size reduction on the other hand. This can be better understood if one considers again a simple model of a bundle of capillary tubes for the porous medium. With this model, the capillary pressure is directly proportional to the IFT and inversely proportional to the tube radius according to

$$P_c = \frac{2\sigma \cos \theta}{r} \quad \dots \dots \dots (2)$$

Keeping the IFT constant, one can readily see that the capillary pressure increase can only result from a decrease of θ (i.e., a wet-

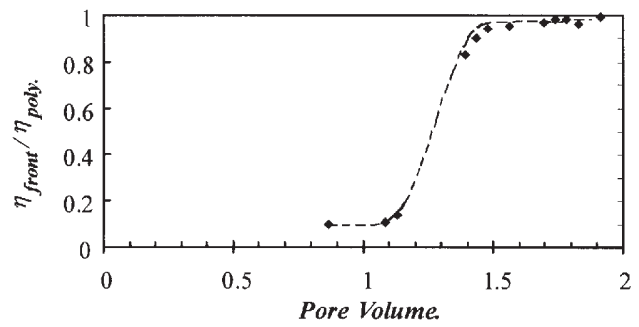


Fig. 4—Propagation of PAM slug in the water-wet medium.

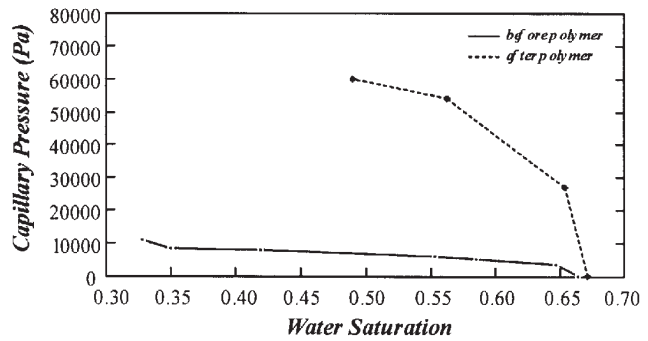


Fig. 5—Capillary pressure as a function of water saturation before and after polymer adsorption in the water-wet core.

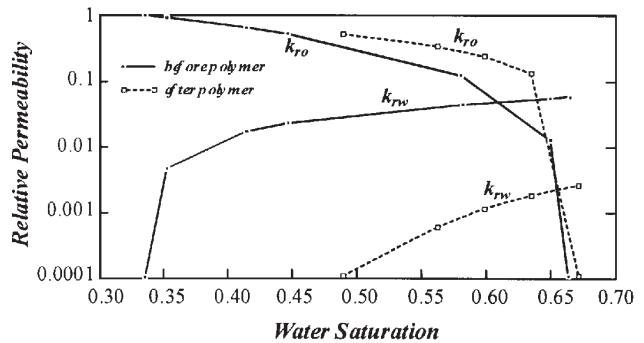


Fig. 6—Modification of water and oil relative permeabilities after PAM injection in the water-wet medium.

tability improvement), which is probably a weak effect in our experiments, and a radius decrease caused by adsorption of the polymer layer. A two-phase-flow numerical study^{7,18} performed on a 2D convergent/divergent model of a porous medium indicates that the presence of an adsorbed layer yields a capillary pressure increase and confirms this physical mechanism from a phenomenological point of view.

Relative Permeabilities. Relative permeabilities are given in Fig. 6. The dimensionless k_r are taken as the ratio of the corresponding effective permeability to the effective permeability to oil at the first irreducible water saturation. The ratio between oil relative permeabilities at endpoints before and after polymer adsorption (k_o at S_{wi}^1 and k_o at S_{wi}^2 , respectively) is equal to 1.6, while the ratio between water relative permeabilities at endpoints (k_w at S_{or}^1 and k_w at S_{or}^3) is equal to 22.1. This result shows a strong selective effect of the polymer adsorbed in the core and is in good agreement with previous works.^{2,3,5} This behavior has also been obtained numerically with our simulator on a simplified 2D model.

As reported by Hawkins and Bouchard,¹⁹ relative permeability hysteresis is frequently observed during successive imbibition cycles. This is usually a result of the change in fluid distribution at the pore level. To check that the relative permeability change before

S_{wi}	0.30
S_{or}	0.366
$k_w, \mu\text{m}^2$	0.0454
$k_o, \mu\text{m}^2$	0.467
S_{wi}	0.316
S_{or}	0.366
$k_w, \mu\text{m}^2$	0.0382
$k_o, \mu\text{m}^2$	0.466
S_{wi}	0.317
S_{or}	0.366
$k_w, \mu\text{m}^2$	0.349
$k_o, \mu\text{m}^2$	0.461

ϕ	0.24
$k_w, \mu\text{m}^2$	0.10
S_{wi}^1	0.32
k_o at $S_{wi}^1, \mu\text{m}^2$	0.278
S_{or}^1	0.54
k_w at $S_{or}^1, \mu\text{m}^2$	0.047
S_{or}^2	0.22
k_w at $S_{or}^2, \mu\text{m}^2$	0.36
S_{wi}^2	0.49
k_o at $S_{wi}^2, \mu\text{m}^2$	0.118
S_{or}^3	0.17
k_w at $S_{or}^3, \mu\text{m}^2$	0.0114

and after polymer adsorption is not just caused by hysteresis effects, three cycles of oil and brine injection without any polymer in the core material were performed. Results given in **Table 2** show that cycle-dependent hysteresis is weak. This confirms that effects observed previously were essentially caused by the presence of polymer in the core.

Saturation Fields. In **Figs. 7 and 8**, experimental and computed evolution of the reduced water saturation S_w^1 and S_w^2 before and after polymer adsorption, respectively, are represented. They were deduced from the following relationship:

$$S_w^{*j} = \frac{(S_w - S_{wi}^j)}{(1 - S_{or}^j - S_{wi}^j)}, \dots, j = 1, 2 \dots \dots \dots (3)$$

Experimental results correspond to the average saturation computed on the 15 straight sections covering the core, while the computed saturations correspond to the result of a numerical simulation performed with the petrophysical properties of the core (measured capillary pressure and estimated relative permeabilities). For the two imbibition cycles (before and after polymer adsorption, respectively), we note a good agreement between experimental and calculated values. Saturation profiles in the absence of adsorbed polymer are more spread out than in its presence; this is again in accordance with a capillary pressure increase. Several experiments were performed with similar water-wet porous media. We always observe the same behavior (i.e., a selective reduction of the relative permeability to water with respect to the relative permeability to oil and a subsequent increase in the capillary pressure).

Oil-Wet Medium. **Table 3** summarizes the experimental endpoints.

Endpoint Saturations. After the first imbibition (Step 4), we obtained a high value of the ROS ($S_{or}^1 = 0.54$). This value decreased significantly after injection of the polymer solution in the core ($S_{or}^2 = 0.22$). After the second drainage (Step 8) the irreducible water saturation was also increased from $S_{wi}^1 = 0.32$ to $S_{wi}^2 = 0.49$. At

the end of the second imbibition, the oil recovery was even higher. The value of the ROS dropped to $S_{or}^3 = 0.17$.

Capillary Pressure. Capillary pressures measured during the two imbibitions (Steps 4 and 9) are plotted in **Figs. 9 and 10**.

The curve in **Fig. 9** is representative of an oil-wet medium because the capillary pressure is negative, while the curve in **Fig. 10**, (after polymer adsorption in the core) is positive, with a higher maximum value. This curve is representative of a water-wet medium in which pore-throat dimensions are reduced by adsorbed polymer. This result is consistent with the increase in oil recovery observed after polymer injection. Adsorption of polymer on the pore walls drives oil away from the surface of the rock to the pore body, thus enhancing oil recovery and modifying the wettability of the core. Broseta *et al.*¹⁴ also observed adsorption of hydrophilic polymers on oil-wet media.

Relative Permeabilities. In **Fig. 11**, we plotted the cross relative permeabilities obtained from the endpoints measured during the two successive imbibition cycles. Because of the very strong shift in both irreducible water saturation and ROS induced by the polymer, it is difficult to compare relative permeability values obtained at endpoints. Indeed, these values have to be compared at the same saturation state of the core.

Saturation Fields. Time evolution of the reduced water saturation throughout the core, before and after polymer adsorption, respectively, is given in **Figs. 12 and 13**. Although experimental points are very spread out, we can notice a straightening up of the saturation fronts after polymer adsorption.

Conclusions

1. An experimental core-flow equipment enabling direct measurement of the capillary pressure and determination of relative permeabilities during oil and water injections was designed to check the effect of adsorbed polymer.

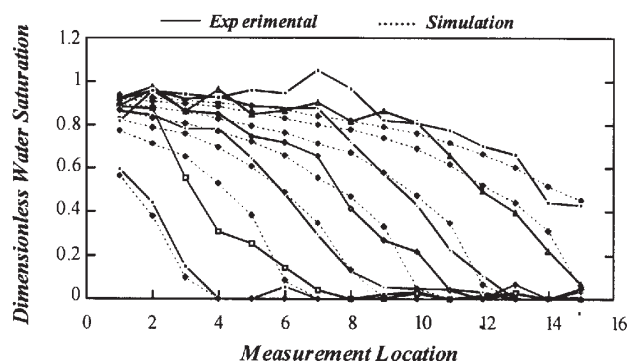


Fig. 7—Waterflooding in absence of adsorbed polymer; comparison between experimental and simulated averaged reduced water saturations.

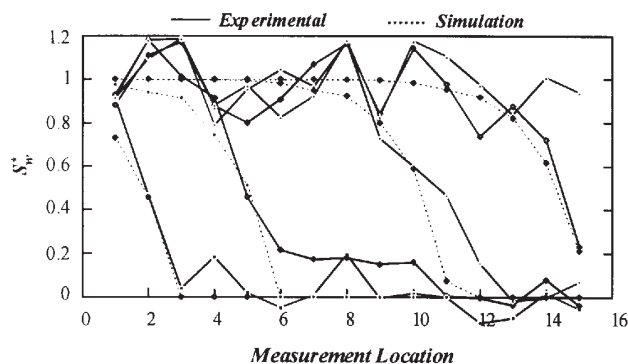


Fig. 8—Waterflooding in presence of adsorbed polymer; comparison between experimental and simulated averaged reduced water saturations.

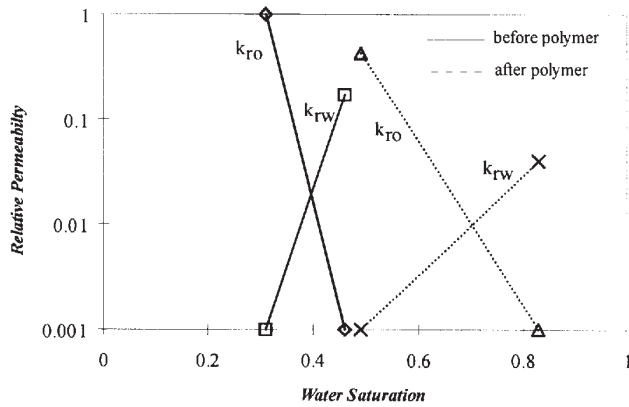


Fig. 9—Modification of water and oil cross relative permeability after PAM injection in the oil-wet medium (endpoints).

2. After polymer adsorption, irreducible water saturation increases. This can be explained partially by the presence in the core of polymer-hydration water, but mainly by the fact that smaller pores are closed to oil flow. This was observed on both water- and oil-wet media. ROS drops significantly after polymer adsorption in oil-wet media, whereas it changes very little in water-wet media.

3. Adsorbed polymer induces a strong increase in the capillary pressure over the whole saturation range. For a water-wet medium, because the polymer does not significantly change the IFT between oil and water, we believe that this effect is mainly the result of the reduction of pore-throat size by the adsorbed-polymer layer and possibly of a (weak) wettability improvement. For an oil-wet medium, a complete change of wettability is observed in addition to pore-size restriction.

4. The change in the relative permeability curves clearly shows the selective action of the polymer, which reduces the relative permeability to water much more than the relative permeability to oil. This effect is stronger with a water-wet than with an oil-wet medium.

5. All these results are consistent with the picture of an adsorbed-polymer layer at pore wall, which modifies considerably the petrophysical properties of the core.¹⁷

Nomenclature

- A = specific area, $L^2/m, m^2/g^{-1}$
- h = thickness of adsorbed polymer layer, $L, \mu m$
- k = absolute permeability, $L^2, \mu m^2$
- k_o = effective permeability to oil, $L^2, \mu m^2$
- k_{ro} = relative permeability to oil
- k_{rw} = relative permeability to water
- k_w = effective permeability to water, $L^2, \mu m^2$
- P_c = capillary pressure, $m/Lt^2, Pa$
- R_k = permeability reduction
- S_{or} = ROS
- S_{or}^1 = ROS (first waterflood)
- S_{or}^2 = ROS after polymer injection
- S_{or}^3 = ROS (second waterflood)
- S_w = water saturation
- S_{wi} = irreducible water saturation
- S_{wi}^1 = irreducible water saturation (first oilflood)
- S_{wi}^2 = irreducible water saturation (second oilflood)
- S_w^{*1} = reduced water saturation (first waterflood)
- S_w^{*2} = reduced water saturation (second waterflood)
- γ = shear rate, $t^{-1}, second^{-1}$
- ϕ = porosity
- η = dynamic viscosity, $m/Lt, mPa \cdot s$
- θ = contact angle, degrees
- σ = IFT, $m/t^2, N/m$

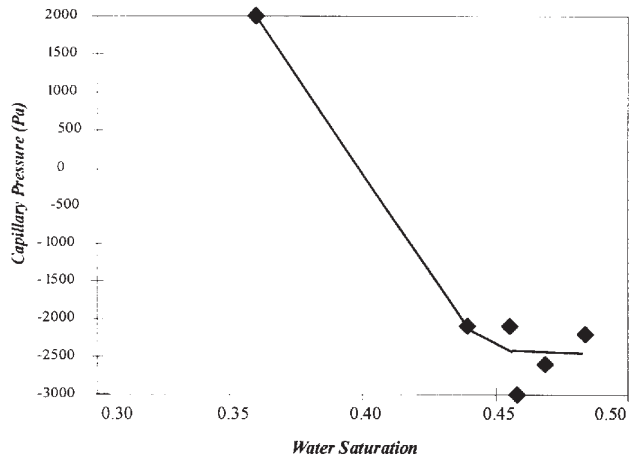


Fig. 10—Capillary pressure as a function of water saturation before polymer adsorption in the oil-wet core.

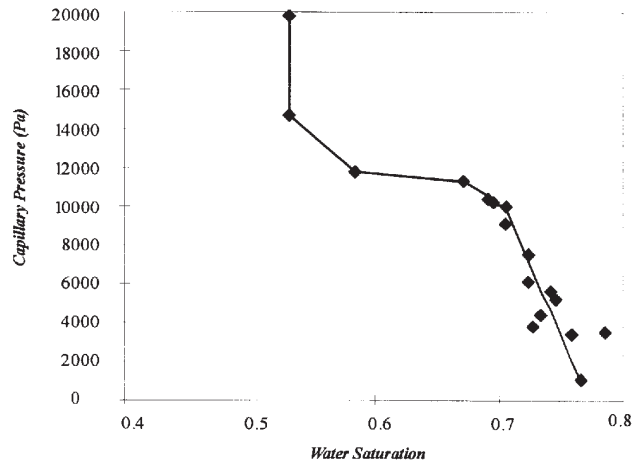


Fig. 11—Capillary pressure as a function of water saturation after polymer adsorption in the oil-wet core.

Acknowledgments

This study was supported by the Groupement Scientifique ARTEP-CNRS, whose financial support is gratefully acknowledged. We thank F. Kalaydjian and G. Lemaire, from Inst. Français du Pétrole (IFP), for helping us design the membrane technique used in this paper to measure the capillary pressure; R. Tabary for fruitful discussions; and L. Rousseau who performed the experiments on the oil-wet medium.

References

1. Mofitt, P.D.: "Long-Term Production Results of Polymer Treatments in Producing Wells in Western Kansas," *JPT* (April 1993) 356.
2. Schneider, F.N. and Owens, W.W.: "Steady-State Measurements of Relative Permeability for Polymer/Oil Systems," *SPEJ* (Feb. 1982) 79.
3. Zaitoun, A. and Kohler, N.: "Two-Phase Flow Through Porous Media: Effect of an Adsorbed Polymer Layer," paper SPE 18085 presented at the 1988 SPE Annual Technical Conference and Exhibition, Houston, 2–5 October.
4. Zaitoun, A., Kohler, N., and Guerrini, Y.: "Improved Polyacrylamide Treatments for Water Control in Producing Wells," *JPT* (July 1991) 862.
5. Liang, J.T., Sun, H., and Seright, R.S.: "Why Do Gels Reduce Water Permeability More Than Oil Permeability?," *SPEJ* (November 1995) 282.
6. Dawe, R.A. and Zhang, Y.: "Mechanistic Study of the Selective Action of Oil and Water Penetrating into a Gel Emplaced in a Porous Medium," *J. Pet. Sci. & Eng.* (December 1994) 12, 113.
7. Barreau, P. *et al.*: "Effect of Adsorbed Polymer on Relative Permeability and Capillary Pressure: A Pore Scale Numerical Study," *BEM XVII*, Brebbia, Kim, Oswald, and Power (eds.), Computational Mechanics Publications, Southampton, U.K. (1994) 549–556.

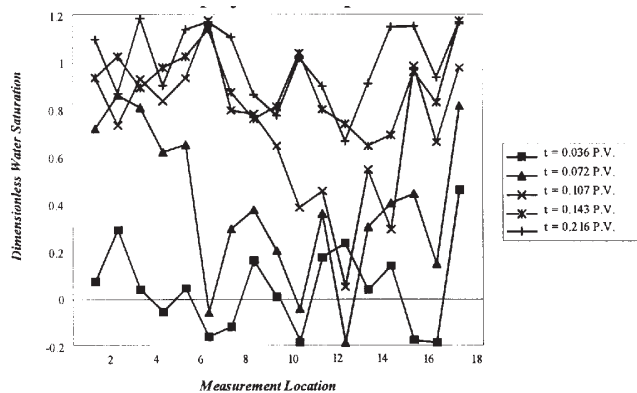


Fig. 12—Waterflooding in absence of adsorbed polymer in the oil-wet core.

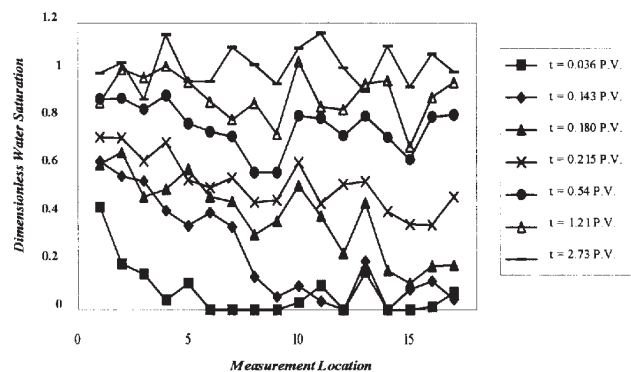


Fig. 13—Waterflooding in presence of adsorbed polymer in the oil-wet core.

8. Barreau, P. *et al.*: "Polymer Adsorption Effects on Relative Permeabilities and Capillary Pressure: Investigation of a Pore-Scale Scenario," paper SPE 37303 presented at the 1997 SPE International Symposium on Oilfield Chemistry Houston, 18–21 February.
9. Barrufet, M.A. and Ali, L.: "Modification of Relative Permeability Curves by Polymer Adsorption," paper SPE 27015 presented at the 1994 Latin/Caribbean Petroleum Engineering Conference, Buenos Aires, 27–29 April.
10. Nicholls, C.I. and Heaviside, J.: "Gamma Ray Absorption Techniques Improve Analysis of Core Displacement Test," *SPEFE* (March 1988) 69.
11. Alhanai, W., Bertin, H., and Quintard, M.: "Two-Phase Flow in Heterogeneous Porous Media, Theoretical and Experimental Results for Nodular Systems," paper SPE 24504 presented at the 1992 Abu Dhabi Petroleum Conference, Abu Dhabi, U.A.E., 18–20 May.
12. Laribi, S., Bertin, H., and Quintard, M.: "Two-Phase Flow Calculations and Comparative Flow Experiments Through Heterogeneous Orthogonal Stratified Systems," *J. Pet. Sci. & Eng.* (January 1995) 12, 183.
13. Lombard, J.M., Lenormand, R., and Robin, M.: "Intermediate Wettability: Capillary Pressure in Mixtures of Oil Wet and Water Wet Sand Grains," *Physical Chemistry of Colloids and Interfaces in Oil Production*, H. Toulhoat and J. Lecourtier (eds.), Technip, Paris (1992).
14. Broseta, D. *et al.*: "Polymer Adsorption/Retention in Porous Media: Effects of Core Wettability and Residual Oil," *SPE Advanced Technology Series* (March 1995) 103.
15. Kalaydjian, F.: "Dynamic Capillary Pressure Curves for Water/Oil Displacement in Porous Media: Theory vs. Experiment," paper SPE 24813 presented at the 1992 SPE Annual Technical Conference and Exhibition, Washington, DC, 4–7 October.
16. Kalaydjian, F.: "Effect of the Flow Rate on an Imbibition Capillary Pressure Curve: Theory vs. Experiment," *Advances in Core Evaluation III Reservoir Management*, P.F. Worthington and C. Chardaire-Rivière (eds.), Gordon and Breach Science Publishers, Amsterdam (1993).
17. Chardaire, C. *et al.*: "Simultaneous Estimation of Relative Permeabilities and Capillary Pressure," paper SPE 19680 presented at the 1989 SPE Annual Technical Conference and Exhibition, San Antonio, Texas, 8–11 October.
18. Chauveteau, G., Tirell, M., and Omari, A.: "Concentration Dependence of the Effective Viscosity of Polymer Solutions in Small Pores with Repulsions or Attractive Walls," *J. Colloids & Interface Sci.* (July 1984) 100, No. 1, 41.
19. Hawkins, J.T. and Bouchard, A.J.: "Reservoir-Engineering Implications of Capillary-Pressure and Relative-Permeability Hysteresis," *Log Analyst* (July–August 1992) 415.

SI Metric Conversion Factors

bbl	× 1.589 873	E-01 = m ³
cp	× 1.0*	E-03 = Pa · s
dyne/cm	× 1.0*	E+00 = mN/m
ft	× 3.048*	E-01 = m
ft ²	× 9.290 304*	E-02 = m ²
°F	(°F - 32)/1.8	= °C
in.	× 2.54*	E+00 = cm
in. ²	× 6.451 6*	E+00 = cm ²
md	× 9.869 233	E-04 = μm ²

*Conversion factor is exact.

Patrick Barreau is a research engineer at Inst. Français du Pétrole (IFP) in Pau, France, where he works on reservoir characterization. Previously, he was a PhD candidate at the U. of Bordeaux, France. **Henri Bertin** is a CNRS researcher in the Laboratoire Energétique et Phénomènes de Transfert-Ecole Natl. Supérieure d'Arts et Métiers (LEPT-ENSAM)—U. of Bordeaux. His research interests are in fluid mechanics in porous media with applications in petroleum engineering (EOR, heterogeneity) and environmental problems. He holds a PhD degree in mechanical engineering from the U. of Bordeaux. **Didier Lasseux** is a CNRS researcher in the LEPT-ENSAM (U. of Bordeaux) working on multiphase/multicomponent flows in porous media at different scales. He holds a BS degree from the ENSAM and a PhD degree from the U. of Bordeaux, both in mechanical engineering. **Philippe Glénat** is a process chemical engineer at Total E&P in Paris. He was previously Head of the Production Chemical Laboratory at the Scientific and Technical Centre of Total E&P. Glénat holds a BS degree in Biochemistry from the Inst. Natl. des Sciences Appliquées, Lyon, France, and a PhD degree in Microbiology from the U. of Lyon. **Alain Zaitoun** is a senior research engineer in the Reservoir Dept. at the IFP. He has worked in polymer flooding and (since 1985) in water control and well treatment. He holds a PhD degree in chemical engineering from the U. of Nancy, France.